2002

Ultrastructure of *Tuzetia weidneri* sp. n. (Microsporidia: Tuzetiidae) in Skeletal Muscle of *Litopenaeus setiferus* and *Farfantepenaeus aztecus* (Crustacea: Decapoda) and New Data on *Perezia nelsoni* (Microsporidia: Pereziidae) in *L. setiferus*

Elizabeth U. Canning
Imperial College

Alan Curry
Withington Hospital

Robin M. Overstreet
Gulf Coast Research Laboratory, robin.overstreet@usm.edu

Acta Protozool. (2002) 41: 63 - 77

ACTA
PROTOZOOLOGICA

Ultrastructure of *Tuzetia weidneri* sp. n. (Microsporidia: Tuzetiidae) in Skeletal Muscle of *Litopenaeus setiferus* and *Farfantepenaeus aztecus* (Crustacea: Decapoda) and New Data on *Perezia nelsoni* (Microsporidia: Pereziidae) in *L. setiferus*

Elizabeth U. CANNING[1], Alan CURRY[2] and Robin M. OVERSTREET[3]

[1]Department of Biology, Imperial College, London, U.K.; [2]Public Health Laboratory, Withington Hospital, Manchester, U.K.; [3]Department of Coastal Sciences, University of Southern Mississippi, Ocean Springs, Mississippi, U.S.A.

Summary. A new microsporidian species, *Tuzetia weidneri* sp. n. , is described from the skeletal muscle of the decapod crustaceans *Litopenaeus setiferus* and *Farfantepenaeus aztecus*. Fresh spores are pyriform, measuring 3.1 x 2.3 µm. All stages have unpaired nuclei. Meronts lie in direct contact with degenerate host cell cytoplasm but produce numerous small blisters at the surface. Multinucleate meronts divide by constriction into groups or chains of uninucleate products. Sporogony is initiated by deposition of a dense surface coat on the plasma membrane of uninucleate or multinucleate stages and fusion of blisters to enclose the sporont in a sporophorous vesicle (SV). Episporontal secretions in the SV are involved in the division of the sporont. During sporogonic division into chains of sporoblasts, the SV divides together with the body of the sporont, so that each sporoblast is enclosed in its own SV. Spores have a flattened anchoring disc that lies in the polar sac, membranous and spongiform regions of the polaroplast and 9-10.5 coils of the isofilar polar tube, around a posterior vacuole. The endospore layer of the spore wall is not thinned over the anchoring disc. The spore wall is adorned with a complex series of ridges. New data are presented on the spores of *Perezia nelsoni* (Sprague 1950) in *L. setiferus*. Of special interest is the polaroplast which is composed of an outer region of tightly-packed membranes in the form of a globule, which almost invariably completely encloses an inner region of loosely packed membranes. The isofilar polar tube, arranged in 8-10 coils angled around the large nucleus in the posterior half of the spore, passes through the membranes of the globular polaroplast near the periphery of the spore, then runs a curved course through the inner polaroplast and passes again through the globular polaroplast to join the anchoring disc. A polaroplast with one region completely enclosed by another has not been described previously.

Key words: *Farfantepenaeus aztecus*, *Litopenaeus setiferus*, Microsporidia, *Perezia nelsoni*, shrimps, taxonomy, *Tuzetia weidneri* sp. n., ultrastructure.

INTRODUCTION

Several microsporidian parasites have been described from shrimps (Crustacea, Decapoda), mostly infecting skeletal muscle and rendering the affected regions opaque white (those recorded before 1971 are listed by Sprague and Couch 1971). Infections may be associated with high mortalities, especially under intensive rearing conditions but, even in the absence of mortality, heavy infections render the shrimp unmarketable and inedible (Overstreet 1973).

Four of these microsporidia have been reported from the penaeid shrimps *Litopenaeus setiferus* (Linnaeus) and *Farfantepenaeus aztecus* (Ives). These are (1)

Address for correspondence: Elizabeth U. Canning, Department of Biology, Imperial College at Silwood Park, Ascot, Berkshire SL5 7PY, U.K.; Fax: +44-0207-594 2339; E-mail: e.canning@ic.ac.uk

Perezia nelsoni (Sprague 1950) Vivarès and Sprague, 1979 (synonyms: *Nosema nelsoni* Sprague 1950; *Nosema pulvis* Jones 1958; *Ameson nelsoni* (Sprague 1950) Sprague 1977); (2) *Thelohania* sp. of Kruse 1959 (also in *Farfantepenaeus duorarum* (*Penaeus duorara*) and considered by Kruse to agree well with *Thelohania duorara* Iverson and Manning 1959); (3) *Pleistophora* sp. of Baxter, Rigdon and Hanna 1970 (synonyms: *Pleistophora penaei* Constransitch 1970, nomen nudum; *Pleistophora penaei* Constransitch 1970 quoted by Couch 1978; *Pleistrophora penaei* of Couch 1983); (4) *Agmasoma penaei* (Sprague 1950) Hazard and Oldacre, 1976 (synonym: *Thelohania penaei* Sprague 1950). The gross appearances of infected hosts have been described by Overstreet (1973) and ultrastructural data are available for *P. nelsoni* (see Sprague and Vernick 1969, Loubès *et al.* 1977, Clotilde-Ba and Togubaye 1996) and *A. penaei* (see Hazard and Oldacre 1976, Clotilde-Ba and Togubaye 1994).

In the genus *Pleistophora* groups of uninucleate spores are formed by sequential division of a multinucleate sporogonial plasmodium within a persistent sporophorous vesicle derived from the surface coat of the sporogonial plasmodium (Canning and Hazard 1982). As part of a study of relationships of *Pleistophora*-like microsporidia from a range of vertebrate and invertebrate hosts, two samples of purified spores were provided by the Gulf Coast Research Laboratory, Ocean Springs, Mississippi for sequencing of the small subunit ribosomal DNA (16S rDNA) at Imperial College, London. The spores, dispersed and non-aggregated after purification, were believed to have been derived from infections of *Pleistophora* sp. and were referred to as *Pleistophora* sp. LS (from *L. setiferus*) and *Pleistophora* sp. PA (from *F. aztecus*) (Cheney *et al.* 2000). In the rDNA study the former sample was found, on sequence data, to be closely related to *Ameson michaelis*, a microsporidium from the crab *Callinectes sapidus*, the only other crustacean host included in the study. *Pleistophora* sp. PA fell into a polytomy with *Glugea atherinae*, *Loma* spp. and *Ichthyosporidium* sp., all parasites of fish. As this study had indicated that the shrimp microsporidia were unrelated to the true *Pleistophora* spp. from fish, an ultrastructural study was undertaken, using tissues from *L. setiferus* and *F. aztecus* infected with a microsporidium with loosely clumped spores as seen in fresh preparations. A second species in *L. setiferus* which gave rise to dispersed spores was also studied.

The results indicated that neither has the generic characters of *Pleistophora*. The microsporidian species with loosely clumped spores was identical in development and spore structure in *L. setiferus* and *F. aztecus*. The morphology has led us to assign it to the genus *Tuzetia* as a new species. This genus has not been reported previously from decapod crustaceans. The microsporidium with dispersed spores was identified as *Perezia nelsoni*. We present a description of the new genus and species as seen in both hosts and provide additional ultrastructural data on *P. nelsoni.*

MATERIALS AND METHODS

Specimens of *L. setiferus* and *F. aztecus* infected with the microsporidia were collected from Davis Bayou and Back Bay of Biloxi, Mississippi, USA. The shrimps were injected into the cephalothorax, hepatopancreas and abdominal musculature with Davidson's fixative (95% ethanol 33 ml, formaldehyde 220 ml, glacial acetic acid 115 ml, distilled water 335 ml) and immersed in the fixative for 3 days before processing tissues for embedding in Paraplast X-tra (53-54°C MP), sectioning at 4 μm and staining with Gill's haematoxylin and eosin (H. and E.). For electron microscopy (EM), small pieces of abdominal muscle and other tissues were fixed in Karnovsky's fixative, washed in 0.1 M cacodylate buffer, postfixed in 1% OsO_4 dehydrated in an ascending series of ethanol solutions and embedded in Spurr's resin *via* propylene oxide. Spores were observed fresh, in Giemsa-stained smears and in histological sections.

RESULTS

Prevalence

Fifty specimens each of *L. setiferus* and *F. aztecus*, collected from the coastal waters, were examined on a monthly basis for microsporidian infection. For several years infections have not exceeded 0.5%.

Tuzetia weidneri sp. n. in *L. setiferus*

Fresh spores (Figs 1, 2) were pyriform, measuring 2.8-4.7 μm (m = 3.31 ± 0.10 μm) x 0.9-3.7 (m = 2.27 ± 0.11 μm). On release from skeletal muscle the spores remained in loose clumps, reminiscent of *Pleistophora* spp. Stained spores (Fig. 3) often showed a dark circle at the broader end. In paraffin sections spores measured 2.2-3.2 μm (m = 2.69 ± 0.05 μm) x 1.4-1.9 μm (m = 1.67 ± 0.05 μm).

Lesions seen in histological sections (Fig. 6) were elongate in the direction of the myofibrils, tapering at the ends. Electron microscopy showed a sharp demarkation between intact muscle fibres (Fig. 8) and the lesions,

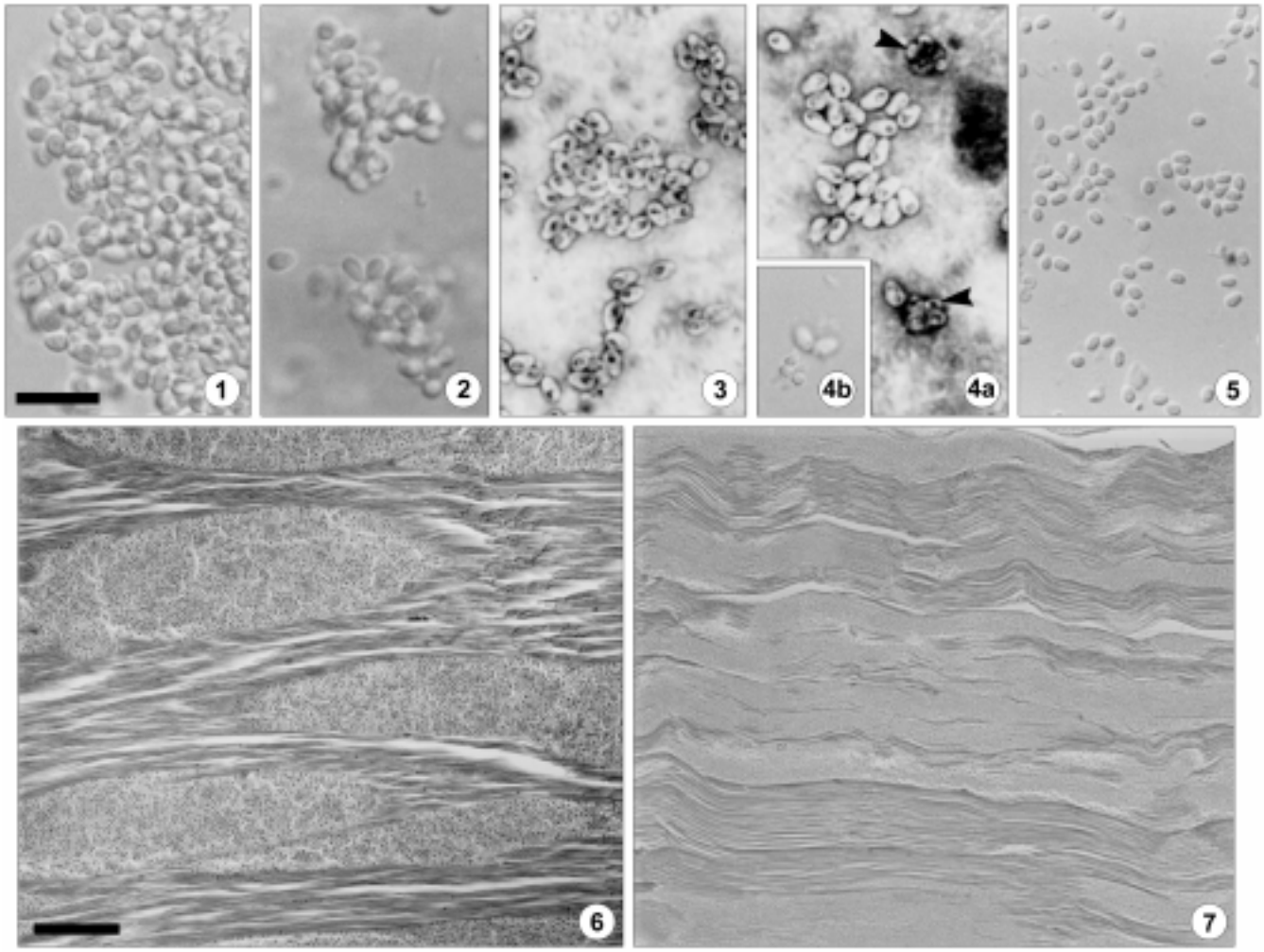

Figs 1, 2. Fresh, pyriform spores of *Tuzetia weidneri* sp. n., released from myocytes in loose clumps. Scale bar on Fig. 1 applies to Figs 2-5. **Fig. 3.** Stained spores of *T. weidneri*, showing darkly stained circle towards the posterior end. **Fig. 4. (a)** Stained spores of *T. weidneri* together with two sporophorous vesicles (arrowheads), each containing eight small spores of a presumed new species. **(b)** Fresh spores of *T. weidneri* adjacent to small spores of a presumed new species. **Fig. 5.** Fresh, ovoid spores of *Perezia nelsoni*, dispersed after release from myocytes. Scale bar - 10 μm (Figs 1-5). **Fig. 6.** Histological section of skeletal muscle of *Litopenaeus setiferus*, stained with H. & E. showing spore-packed lesions with tapering ends, due to *Tuzetia weidneri*. Scale bar on Fig. 6 applies to Fig. 7. **Fig. 7.** Heavily - infected muscle of *L. setiferus* stained with H. & E. showing extensive replacement of muscle fibres by *Perezia nelsoni*. Note more uniform appearance of the lesions than those caused by *T. weidneri*. Scale bar - 100 μm (Figs 6, 7)

which were packed with spores and stages of merogony and sporogony. Within the spore masses, there were a few bundles of frayed myofibrils in otherwise disorganised host cell cytoplasm, with abundant vesicles and occasional myocyte nuclei and cristate mitochondria. Chromatophores of the host produce a gross bluish-black colouration in response to infection.

Membrane systems were not well preserved within parasites apart from the nuclear envelope in some individuals. Meronts were multinucleate plasmodia bounded by a simple plasma membrane (Fig. 9). These became lobed, then elongate and divided by cytoplasmic contriction into groups or chains of multinucleate, binucleate, and ultimately, uninucleate products (Fig. 10). Nuclei contained dense mats of chromatin. Occasionally cytoplasmic preservation was good enough to reveal some cisternae of endoplasmic reticulum (Fig. 12). The surface of all merogonic stages was beset with a multitude of tiny blisters, some in contact with the plasma membrane (Fig. 9, insert), others detached and extended into the surrounding disorganised host tissue (Fig. 11). Division was effected by invagination between segments of cytoplasm containing nuclei. In the planes of division typical blisters were interspersed with larger,

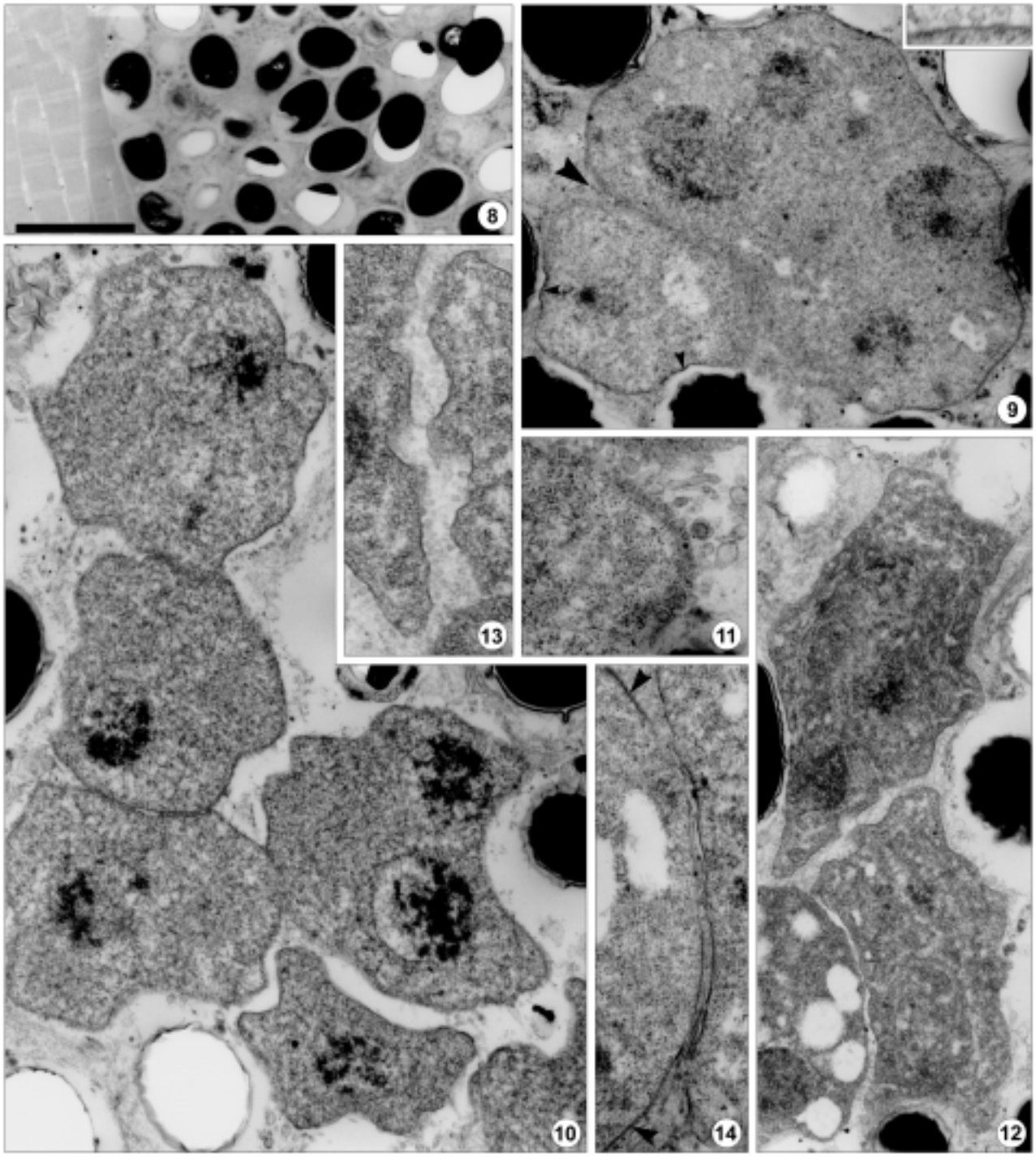

Figs 8-14. Electron micrographs of *Tuzetia weidneri* in skeletal muscle of *Litopenaeus setiferus*. Scale bar on Fig. 8 applies to all figures. **8.** Section at edge of lesion, showing intact muscle bordering spores in individual SVs, isolated in degraded host cell cytoplasm. **9.** Multinucleate meront at the onset of division: surface blisters are abundant in the division plane (arrowhead). Some areas show the first signs of deposition of surface coat (small arrowheads). The insert shows blister formation from the plasma membrane of a meront. **10.** Merogony in progress, giving rise to a chain of uninucleate products. **11.** Part of the surface of a multinucleate meront showing abundant attached and separate surface blisters. **12.** Newly separated products of merogony with restoration of surface blisters between the pair. **13.** Enlargement of part of Fig. 12 showing surface blisters. **14.** Division plane in merogony showing fusion of surface blisters and newly secreted tiny blisters (arrowheads). Scale bar: Fig. 8 - 4.0 μm; Fig. 9 - 0.2 μm and 0.06 μm (insert); Fig. 10 - 1.2 μm; Fig. 11 - 0.6 μm; Fig. 12 - 1.4 μm; Figs 13, 14 - 0.8 μm

elongate vesicles, and minute, apparently newly-formed blisters were present on the plasma membranes (Fig. 14). When daughter meronts were more widely separated, abundant new blisters were present between

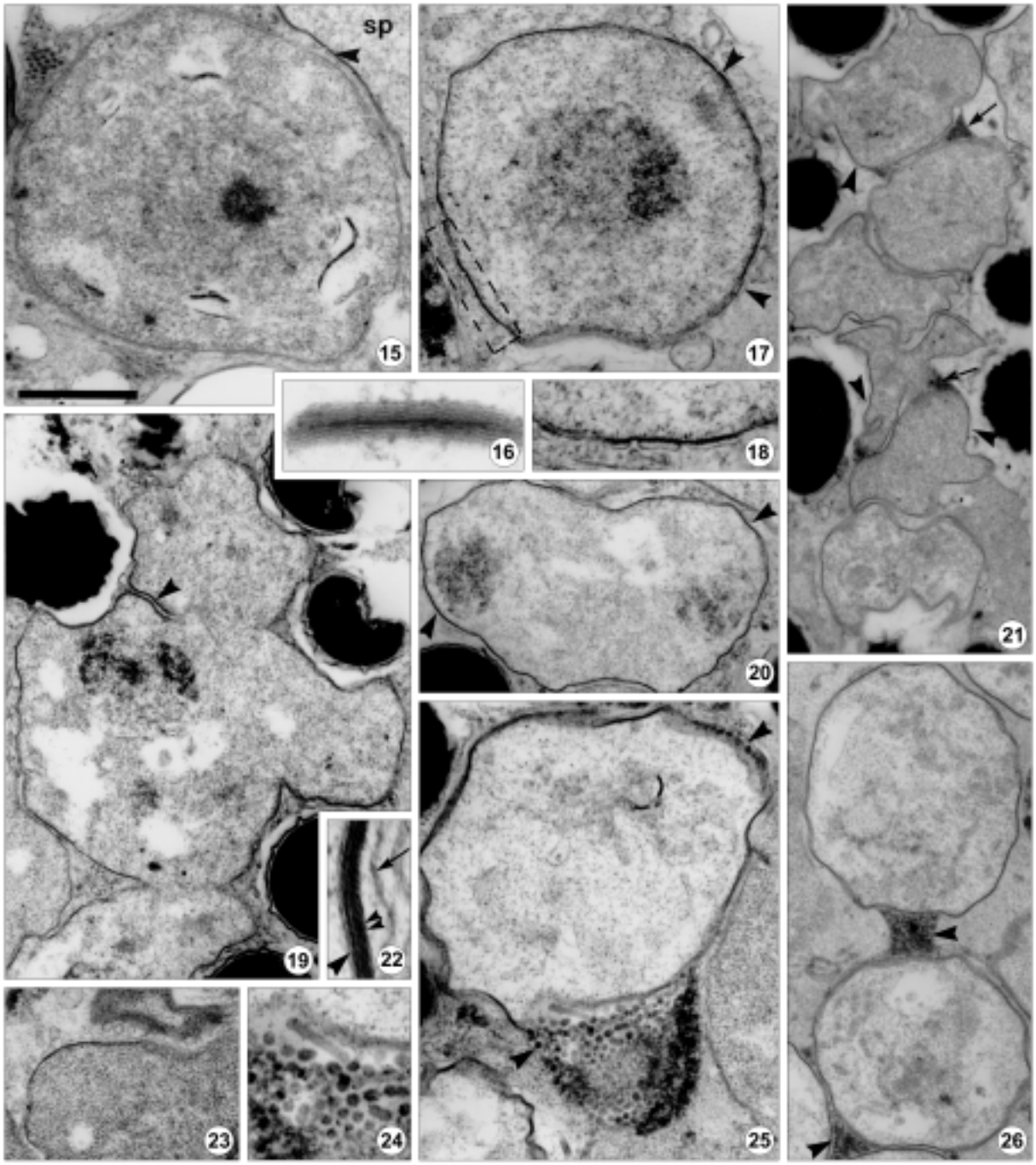

Figs 15-26. Electron micrographs of sporogony of *Tuzetia weidneri* in *Litopenaeus setiferus*. Scale bar on Fig. 15 applies to all figures. **15.** Incipient sporont, product of merogony, with several dense stacks of membrane in the cytoplasm. An adjacent sporont (sp) shows surface coat deposition and partial SV formation (arrowhead). **16.** Detail of membrane stack in sporont cytoplasm. **17.** Uninucleate sporont showing fusion of surface blisters during formation of SV (arrowheads). The boxed area is enlarged in fig. 18. **18.** Enlargement of boxed area of fig. 17 showing surface coat and fusion of blisters to form the SV. **19.** Division of sporont with moderately thick surface coat, while SV is incomplete: surface blisters are fusing in the division plane (arrowhead). **20.** Within a chain, a binucleate product of sporogony with well developed surface coat and complete SV (arrowheads). **21.** Chain of sporoblasts derived from sporogony. Individual SVs (not always clear) are indicated at arrowheads. Episporontal secretions lie in the division planes (arrows). **22.** Surface characteristics of mature sporont: the SV envelope (arrow) overlies the thick surface coat (small double arrowheads) on plasma membrane (arrowhead). The second SV belongs to an adjacent sporont. **23.** Part of the surface of an early multinucleate sporont showing deposition of surface coat prior to complete fusion of surface blisters. **24.** Enlargement of episporontal secretions from fig. 25. **25.** Sporont with complete SV and with episporontal tubules and globules accumulated in two patches (arrowheads). **26.** Formation of sporoblasts: accumulation of episporontal secretions (arrowheads) between sporoblasts during constriction of the SV envelope around individuals. Scale bar: Fig. 15 - 0.6 μm, Figs 16, 19, 20, 22, 26 - 1.2 μm; Figs 17, 23, 25 - 0.8 μm; Figs 18, 24 - 0.4 μm; Fig. 21 - 1.6 μm

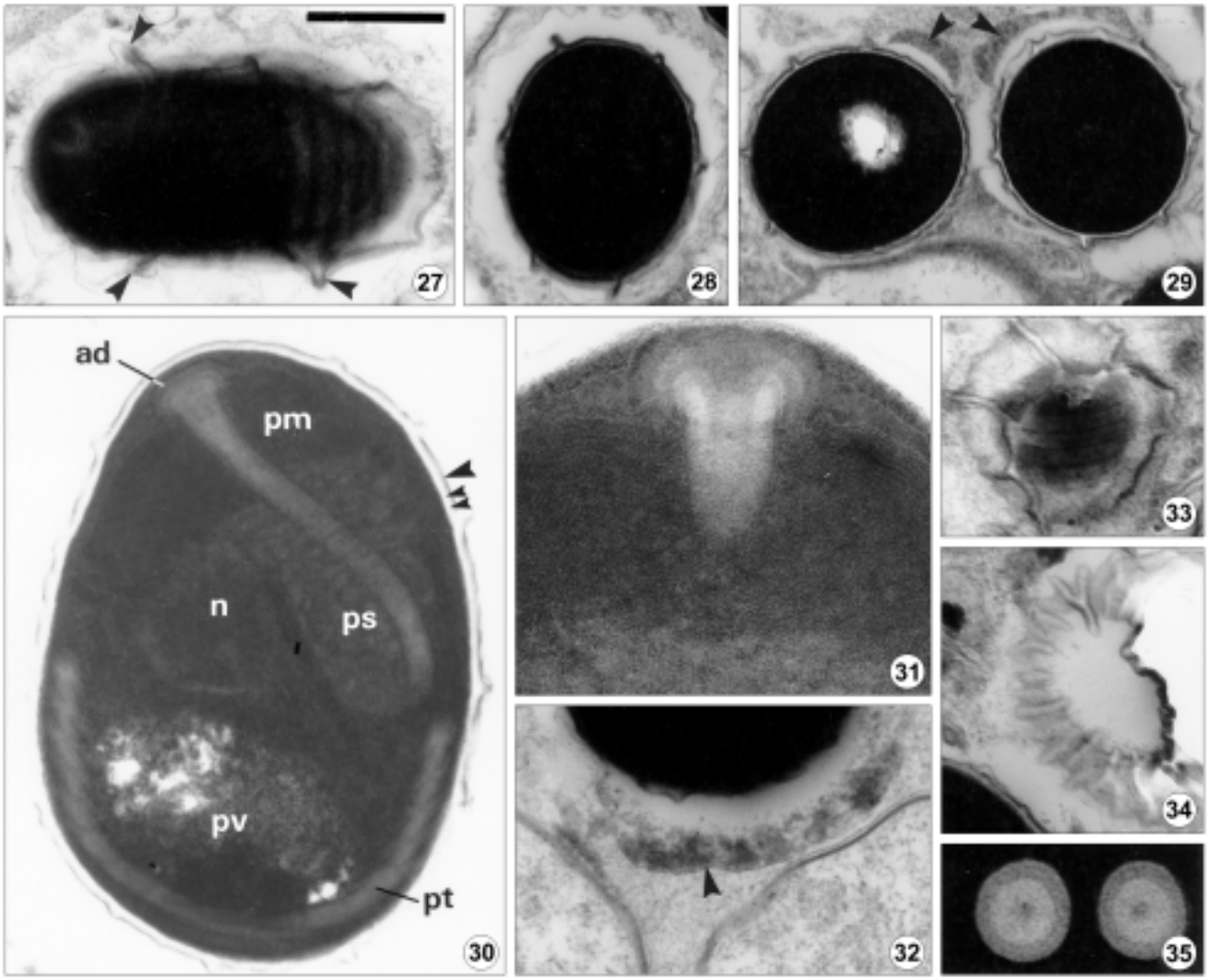

Figs 27-35. Electron micrographs of spores of *Tuzetia weidneri* in *Litopenaeus setiferus*. Scale bar on Fig. 27 applies to all figures. **27.** Longitudinal section of mature spore showing ridges of the spore wall (arrowheads) in contact with SV envelope. SV lacks episporontal secretions. **28.** Oblique section of mature spore, with ridged wall, in SV devoid of episporontal secretions. **29.** A pair of spores, possibly within a single SV containing degraded episporontal secretions (arrowheads). **30.** Mature spore showing exospore (arrowhead) with ridges, endospore (small double arrowheads), anchoring disc (ad), membranous polaroplast (pm), spongiform polaroplast (ps), polar tube (pt), nucleus (n) and posterior vacuole (pv). **31.** Detail of anchoring disc with several layers of differing density, into which the central tube of the polar tube spreads like a funnel. **32.** Part of SV containing a mature spore: the episporontal tubules and globules have been degraded (arrowhead) but not yet eliminated. **33, 34.** Sections of spores tangential to parts of the spore wall showing surface ridges, some of which are branched. Part of the polar tube is visible in Fig. 33. **35.** Transverse sections of polar tube coils showing concentric rings around a central core. Scale bar: Figs 27, 32-34 - 0.6 µm; Figs 28, 29, 35 - 1.0 µm; Fig. 30 - 0.4 µm; Fig. 31 - 1.8 µm

them (Fig. 13), possibly expanded from the tiny blisters seen in Fig. 14.

Uninucleate products of merogony, were incipient sporonts, and many showed stacks of membranes in the cytoplasm (Figs 15, 16) which persisted in some specimens during conversion to sporonts (Fig. 25)

Sporonts were recognised by the presence of an electron dense surface coat on the plasma membrane and a sporophorous vesicle (SV), which appeared to be formed by progressive coalescence of the blisters at the meront surface (Figs 17, 18). The initiation of sporogony was observed in both uninucleate (Fig. 17) and multinucleate (Fig. 19) products of merogony. These showed varied surface characters, parts of the surface being typical of meronts with a simple plasma membrane and abundant blisters and other parts covered with a thin surface coat and discontinuous SV envelope formed by coalescence of blisters (Fig. 23). When mature, the sporont surface coat was a 20 nm layer directly overlying the plasma membrane, outside of which was the

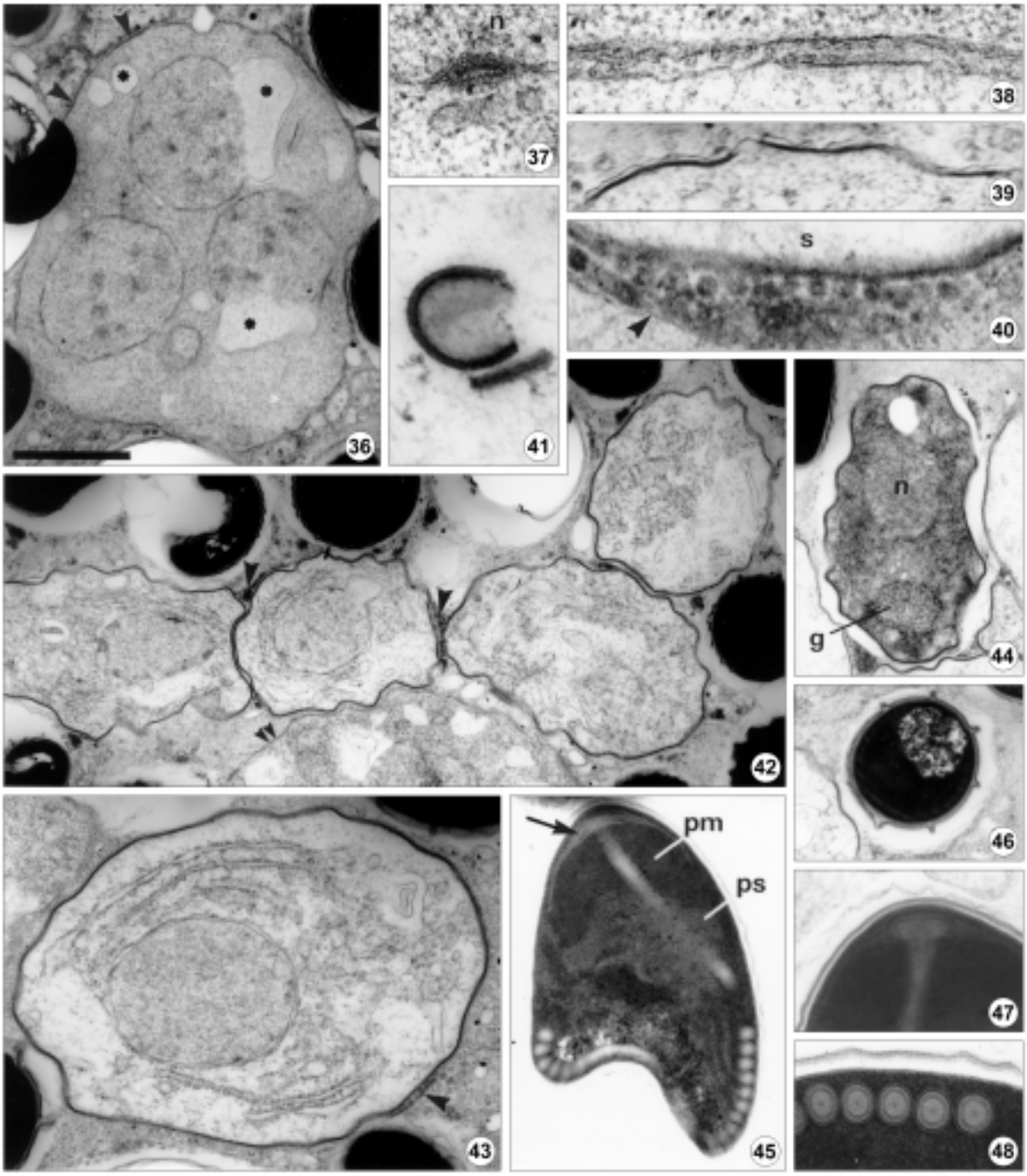

Figs 36-48. Electron micrographs of *Tuzetia weidneri* from skeletal muscle of *Farfantepenaeus aztecus*. Scale bar on Fig. 36 applies to all figures. **36.** Incipient sporont. Cytoplasmic vacuoles and expansions within the nuclear envelope*, containing a network of fine granules appear abnormal. The plasma membrane bears minute blisters (arrowheads). **37.** Spindle pole within the nucleus (n) of a multinucleate meront, showing electron dense discs and vesicles external to the spindle terminus. **38.** Division plane between products of merogony showing small blisters. **39.** Surface of developing sporont showing areas of unthickened plasma membrane and areas where the surface coat has been deposited and surface blisters have fused during formation of the SV. **40.** Surface of an early sporont (s) with episporontal secretions within the SV envelope (arrowhead). **41.** Stacks of membranes in the cytoplasm of an early sporont. **42.** Chain of uninculeate sporoblasts formed by constriction of a sporont. Episporontal secretions accumulate within the SV at the points of constriction (arrowheads). An adjacent meront has minute surface blisters (small arrowheads). **43.** Newly isolated sporoblast, with thick surface coat, enveloped in its own SV. Some episporontal secretions persist (arrowhead). **44.** Crenated sporoblast in SV. The nucleus (n) and Golgi vesicles (g) are visible. **45.** Mature spore showing exospore and endospore, polar sac (arrow) extending over membranous polaroplast (pm), polar tube running through spongiform polaroplast (ps) and coiling around the posterior vacuole. **46.** Section of a mature spore, passing through the posterior vacuole, showing ridged spore wall and SV devoid of secretions. **47.** Anterior end of mature spore showing anchoring disc with layers of differing density, through which the central tube of the polar tube opens like a funnel. **48.** Transverse sections of polar tube showing lucent and grey rings and double sleeve around a central core. Scale bar: Figs 36, 44 - 1.2 µm; Figs 37-41, 48 - 0.2 µm; Figs 42, 46 - 1.4 µm; Figs 43, 45, 47 - 0.8 µm

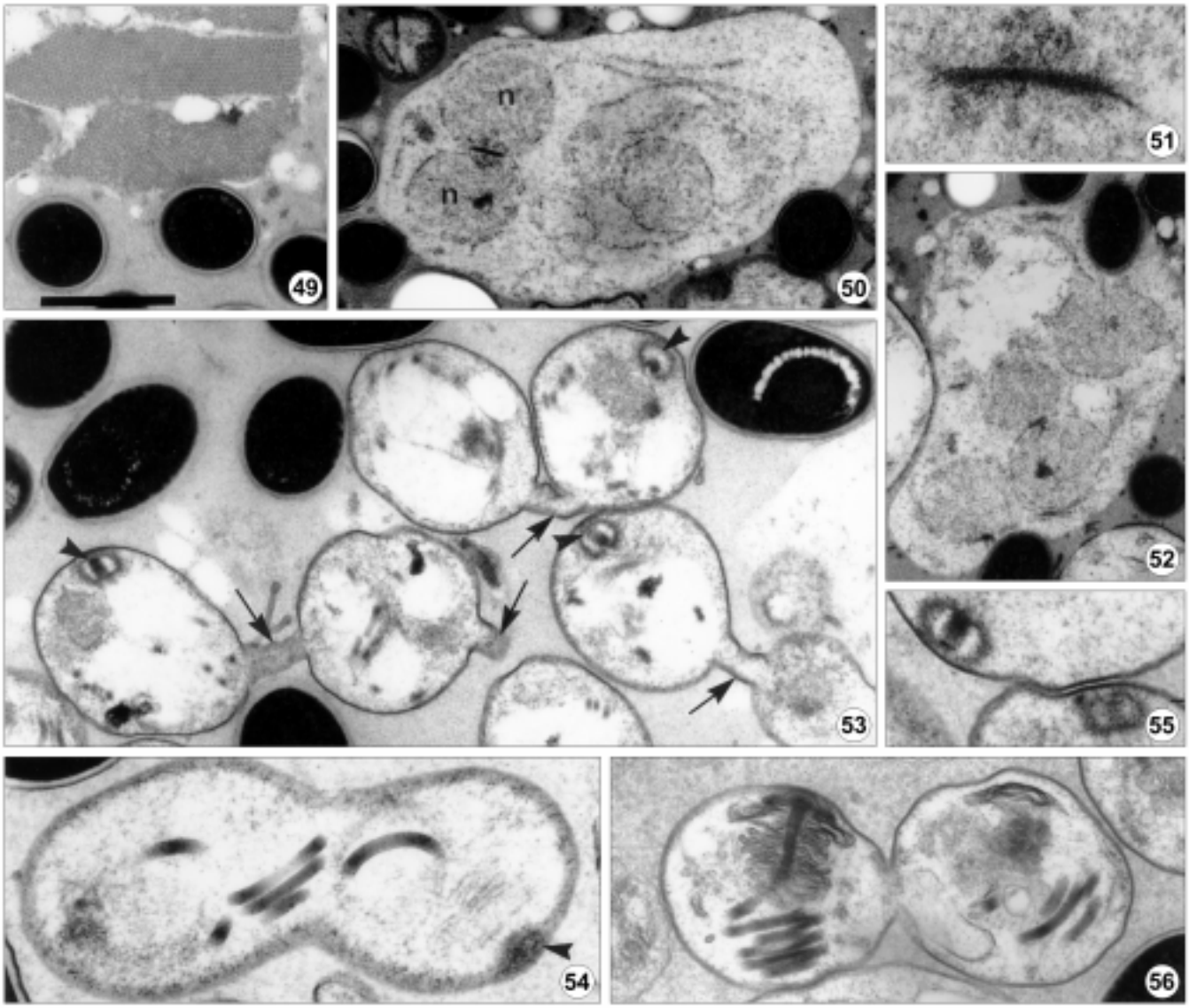

Figs 49-56. Merogony and sporogony of *Perezia nelsoni* in skeletal muscle of *Litopenaeus setiferus*. Scale bar on Fig. 49 applies to all figures. **49.** Intact muscle bundles, at the edge of skeletal muscle lesion and spores in an amorphous matrix of totally degraded muscle. **50.** Meront showing two nuclei (n) in diplokaryotic arrangement with very dense apposition of the four membranes of the nuclear envelopes. One nucleus of another pair is also visible. **51.** The very dense apposition of diplokaryotic nuclei in a meront. **52.** Separation of diplokaryotic nuclei in a meront in preparation for sporogony. **53.** Sporogonic division by binary or multiple fission. The sporoblasts are connected by narrow bridges (arrows). The developing anchoring discs are seen in three of the sporoblasts (arrowheads), in these cases directed away from the region of fission. **54.** Binary fission of a sporont showing coils of the polar tube near the constriction of the body and an anchoring disc at one pole (arrowhead). **55.** The point of separation of two sporoblasts showing the anchoring discs directed towards the plane of fission. **56.** Separation of two sporoblasts showing the long axis, indicated by the anchoring disc, polaroplast and polar tube, parallel to the plane of fission. Scale bar: Fig. 49 - 1.2 μm; Figs 50, 52 - 1.6 μm; Fig. 51 - 0.4 μm; Fig. 53 - 1.0 μm; Fig. 54 - 0.6 μm; Fig. 55 - 0.56 μm; Fig. 56 - 0.9 μm

SV envelope which measured 4.0 nm (Fig. 22). The SV envelope was separated from the surface coat by an irregular episporontal space (Fig. 22).

Once surface coat and SV formation had been completed, sporonts appeared less dense than meronts, with fewer ribosomes, and secretions were observed in the SV cavity (episporontal space). These took the form of 45-50 nm globules or short tubules with a slightly less dense centre (Figs 24, 25). Sporogonic divisions were by binary or multiple fission (Figs 19, 21), giving rise to groups or chains of uninucleate products, sometimes via binary fission of binucleate products within the chain (Fig. 20). The secretions in the episporontal space clearly had a role in the division process, as they were

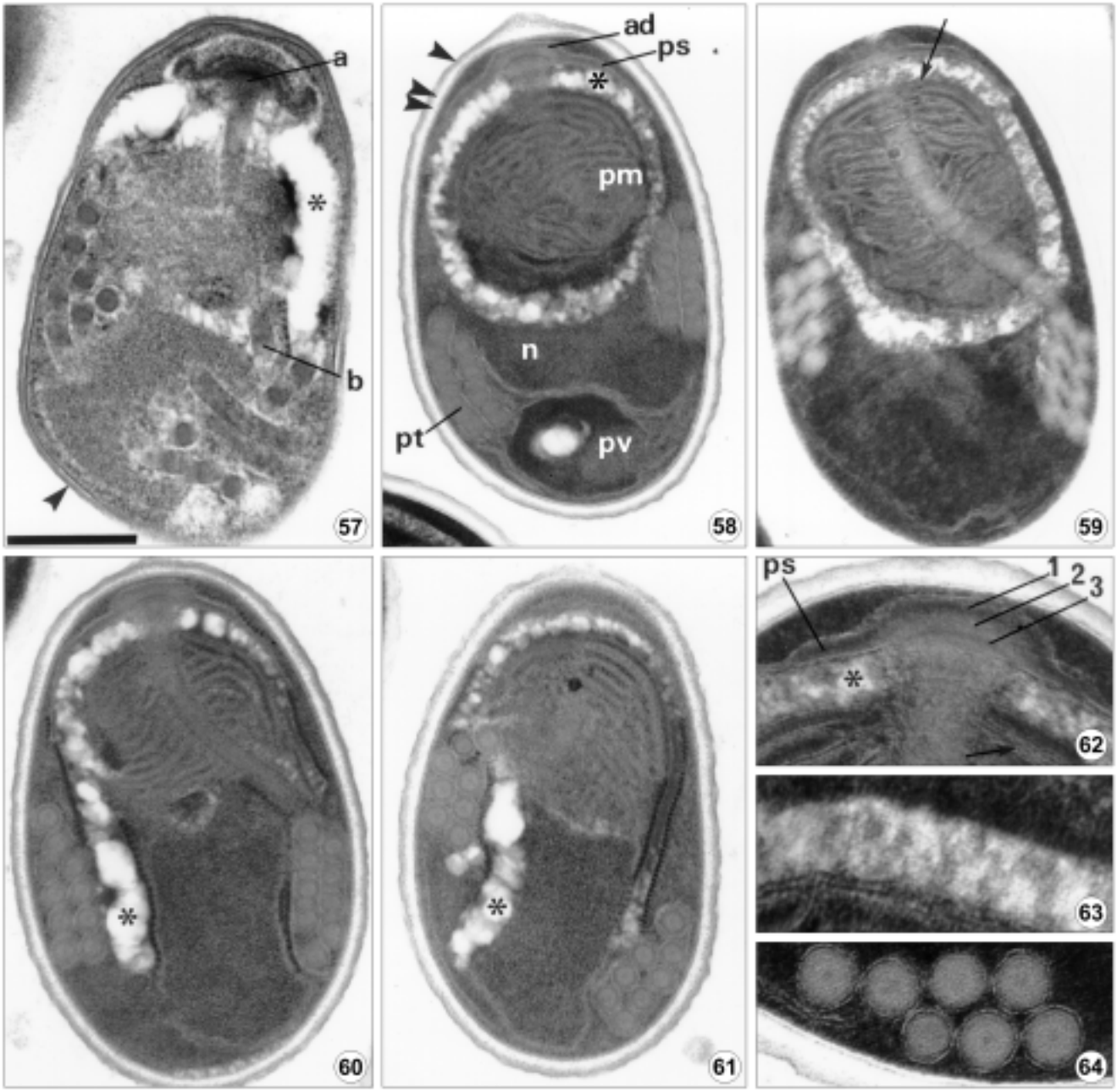

Figs 57-64. Spores of *Perezia nelsoni* in skeletal muscle of *Litopenaeus setiferus*. Scale bar on Fig. 57 applies to all figures. **57.** Immature spore with thick exospore (arrowhead) and minimal endospore layers of the wall. The outer polaroplast region* (appearing empty) forms a globular sac penetrated anteriorly by the polar tube for its attachment (a) to the anchoring disc and posteriorly at the point where the curved part of the tube joins the coil (b). **58.** Mature spore showing thick exospore (arrowhead), endospore (double arrowhead), anchoring disc (ad) within the polar sac (ps), outer region of the polaroplast in the form of a globule (*), inner polaroplast region of widely spaced membranes (pm), nucleus (n), polar tube coils (pt) and posterior vacuole (pv). **59.** Mature spore: section cut laterally to the median sagittal plane, showing the anterior part of the polar tube passing through the inner and outer polaroplast regions to unite with its coil. A few closely packed membranes lie at the anterior border of the inner polaroplast (arrow). **60.** Slightly oblique section of mature spore showing the anchoring disc, straight and coiled regions of the polar tube. The outer, lucent, component of the polaroplast (*) appears as an open structure surrounded by prominent polyribosomes. Compare with fig. 59. **61.** Mature spore: section cut laterally to the median sagittal plane so that the anchoring disc and straight part of the polar tube are not visible. The outer, lucent, component of the polaroplast (*) appears as an open structure surrounded by polyribosomes. **62.** Anterior end of mature spore: the endospore is not thinned over the anchoring disc, which has a dense anterior border (1) continuous with the polar sac (ps), a middle less dense region (2) and a fine inner layer (3) over the insertion of the polar tube. The polar tube passes through a narrow opening in the outer polaroplast region (*) in which traces of parallel membranes can be seen. A few membranes of the inner polaroplast (arrow) are tightly packed. **63.** Section through the outer region of a mature spore showing parallel membranes in the outer polaroplast region. **64.** Transverse sections through coils of the polar tube showing outer sleeve of two membranes and inner rings round a central core. Scale bar: Figs 57-61 - 0.4 μm; Figs 62, 64 - 0. 2 μm; Fig. 63 - 0.1 μm

present only in the narrow channels formed by constriction of the SV envelope between division products, before the final isolation of each sporoblast in its own SV (Figs 21, 26).

Sporoblasts matured into spores but the full sequence of events was not tracked. The episporontal secretions were broken down during spore maturation (Figs 29, 32) and were absent from most SVs containing mature spores. After maturation, each spore lay in its individual SV (Figs 27, 28). Occasionally a pair of spores appeared to be in the same SV (Fig. 29) but this may have resulted from breakdown of the SV in the heavy infection. The spores were pyriform (Fig. 30) although the posterior end had often collapsed during EM fixation (Fig. 8). The anchoring disc within the polar sac was slightly offset from the longitudinal axis and was separated from the spore wall by a 20 nm band of cytoplasm. The anchoring disc was composed of several layers decreasing in density in a posterior direction (Fig. 31). The polar tube abutted on to the last layer, while an inner component of the tube appeared to expand like a funnel through the layers (Fig. 31). The polar sac spread umbrella-wise over about half of the membranous region of the polaroplast. The polaroplast consisted of an anterior region of very tightly packed membranes occupying almost the width of the spore and about a fifth of its length, followed by a spongiform region which surrounded the polar tube during its course from a central to a peripheral position, and was thereby displaced laterally when viewed with the curve of the tube (Fig. 30). The nucleus lay alongside the spongiform polaroplast. The polar tube ran an oblique course through the two regions of polaroplast and formed 9-10.5 isofilar coils in a single layer in the posterior half of the spore, around a voluminous posterior vacuole containing flocculent material. In transverse section the coils of the polar tube showed a central dot surrounded successively by a lucent ring, a grey ring containing longitudinally running fibrils and two membranes (Fig. 35). The endospore measured 20-30 nm and was hardly thinned over the anchoring disc. The exospore was a 20 nm finely granular layer. The two layers were raised as complex branching and anastomosing system of ridges which appeared as protrusions in both longitudinal (Fig. 27), oblique (Fig. 28) or transverse sections (Fig. 29). Tangential sections across the spore surface revealed the complexities of the ridges (Figs 33, 34). At maturity spores usually lay free in the SV but in some cases the SV envelope made contact with the ridges on the spore wall (Fig. 27) and the episporontal space was usually devoid of secretions (Figs 27, 28). In heavily infected tissues many of the SV envelopes had broken down leaving spores dispersed in degraded host cell cytoplasm.

Tuzetia weidneri* sp. n. in *F. aztecus

Lesions in skeletal muscle were similar to those in *L. setiferus*, with total destruction of muscle fibres, leaving only remnants of cytoplasmic organelles. The bluish-black colouration of infected shrimps was observed as in *L. setiferus*. Preservation of parasite membrane systems was better than in *L. setiferus*, although large vacuoles containing an apparently abnormal network of fine granules were common in all stages. Some of these vacuoles were in the cytoplasm and others were clearly in part of the nucleus, lying internal to the nuclear envelope (Fig. 36). Centriolar plaques at spindle poles showed 2 or 3 associated external vesicles (Fig. 37). Surface blisters were less abundant but were present on meronts as a single layer and were involved in meront division (Fig. 38). Transition to sporogony involved secretion of the surface coat and progressive fusion of blisters to form the SV envelope (Fig. 39). Sporonts also exhibited the characteristic features of decreased electron density, aggregates of episporontal secretions in the SV (Fig. 40) and presence of multilamellar bodies in the cytoplasm (Fig. 41). Sporogonic divisions involved a series of fissions with the episporontal secretions positioned in the cytoplasmic fission planes (Fig. 42). Each sporoblast was finally enveloped in its own SV (Fig. 43). During maturation, sporoblasts showed a wavy or crenated outline, a single nucleus and a prominent Golgi apparatus of convoluted tubules in a posterior position (Fig. 44).

Spores, each lying in a persistent SV, were pyriform, often with the posterior end collapsed inwards (Fig. 45), and showed an anchoring disc with the same arrangement of layers (Fig. 47) as the species in *L. setiferus*, membranous and spongiform vesicular regions of polaroplast, the latter being laterally displaced (Fig. 45), around the polar tube along its curve toward the spore periphery. There was a single nucleus, 9 to 10.5 isofilar coils of the polar tube and a posterior vacuole with flocculent contents. Sections of the polar tube showed the same layers as in the parasites in *L. setiferus* (Fig. 48). The endospore measured 20 nm, with only slight thinning over the anchoring disc and the exospore

was a finely granular layer. The wall was raised into prominent ridges visible in all planes of section (Fig. 46).

Octosporous species

Among the masses of large spores of *T. weidneri*, much smaller spores measuring less than 2.0 x 1.0 µm were occasionally encountered (Fig. 4b). These had been released from groups of 8 in SVs (Fig. 4a). It is likely that these represent yet another microsporidian species infecting penaeid shrimps, rather than a stage of the *T. weidneri*, but their very rare occurrence prevented us from obtaining ultrastructural data.

Perezia nelsoni* from *L. setiferus

Fresh spores released from muscle were almost perfectly ellipsoid, measured 1.4-2.8 µm (m = 2.1 ± 0.07) x 0.9-1.9 µm (m = 1.22 ± 0.06) (N = 30) and were dispersed on release from muscle with no evidence of clumping (Fig. 5). Histological sections of skeletal muscle (Fig. 7) showed extensive lesions which appeared more homogeneous than those caused by *T. weidneri* (Fig. 6), probably because of the small spore size. Spores in sections measured 1.4-2.3 µm (m = 1.9 ± 0.4 µm) x 0.9-1.6 µm (m = 1.37 ± 0.04 µm). Data from light microscopy of this species in *F. aztecus* are similar. Electron microscopy showed that the lesions in skeletal muscle were packed with spores interspersed with developmental stages in an amorphous, homogeneous, finely granular background that formed a matrix virtually devoid of host cell organelles, indicating that the degradation of host cell cytoplasm was more complete than in lesions caused by *T. weidneri*. At the edges, the myofibrils were intact (Fig. 49) or only partially degraded. Infected hosts turned bluish-black.

Fixation of meronts and sporonts was poor, with clear spaces in the cytoplasm and minimal preservation of nuclear and cytoplasmic membranes. Meronts, in direct contact with the amorphous host cell matrix, were multinucleate, with simple plasma membrane and diplokaryotic nuclei (Fig. 50). In the plane of apposition of the diplokarya, the nuclear envelopes were exceptionally dense (Fig. 51). The nuclei separated from one another in preparation for sporogony (Fig. 52). After secretion of the electron dense surface coat on the plasma membrane sporonts underwent a series of divisions by binary or multiple fission (Fig. 53) to produce uninucleate sporoblasts. A number of these were connected by cytoplasmic bridges which were presumed to be temporary. Most micrographs suggested that pairs of sporoblasts were separated as mirror images with the anchoring discs directed away from the constricting cytoplasm and the coils of the polar tube close to the constriction (Figs 53, 54) but this arrangement could be reversed with anchoring discs near the division plane (Fig. 55). Arrangement of the anchoring discs, polaroplast membranes and polar tubes in some dividing stages indicated that the longitudinal axis could also be at right angles to the constriction (Fig. 56).

Preservation of immature (Fig. 57) and mature spores (Figs 58-61) was good except for the outer polaroplast membranes. The exospore was finely granular usually about 20 nm thick (Figs 58, 60) but sometimes only 10 nm (Fig. 62). The lucent endospore, about 25-35 nm thick, was only slightly thinned at the anterior end (Fig. 60). The anchoring disc was a flattened structure with its unit membrane separated by a 10 nm layer of cytoplasm from the plasma membrane (Figs 58, 62). The disc, made up of dense anterior and posterior layers with a middle, less dense layer, was continuous with the polar sac which extended over one third to one half of the polaroplast. The polar tube was inserted into the base of the anchoring disc. It then traversed the polaroplast obliquely towards the periphery. In the vast majority of spores, the outer part of the polaroplast in median sagittal sections appeared as a bright ring composed of granular material in a lucent background (Fig. 58). However, parts of the organelle showed traces of parallel membranes (Fig. 63). The ring structure appeared complete whether viewed in transverse or longitudinal section, even in sagittal sections lateral to the median, which showed the connection between the anterior part of the polar tube and the coils (Fig. 59). This outer part of the polaroplast was interpreted as a globular structure with a narrow anterior opening through which the polar tube passed to join the anchoring disc (Fig. 58). At the posterior end the membranes forming the globular polaroplast, were breached again by the polar tube where it passed between its curved section inside, and the coiled section in the posterior half of the spore (Fig. 59). Very occasionally the outer polaroplast was open to the rest of the spore (Figs 60, 61). Within the globular structure were typical polaroplast membranes, of which the 4-8 most anterior membranes, often visible on one side only (Figs 59, 62), were very closely packed and the remainder, almost filling the globule, were separated by a 25 nm dense matrix (Figs 58, 59).

The single large nucleus (Figs 58, 60, 61) lay immediately posteriad of the globular polaroplast and behind this was a posterior vacuole (Fig. 58), which was membrane-bound, with granular contents. The isofilar polar tube was arranged in a tight cluster of two layers of coils. Each showed a dense core and several layers

within a double membrane sleeve (Fig. 64). The number of coils ranged from 8 to 10. Prominent rows of ribosomes were sometimes seen along the borders of the "globular" polaroplast when present as an open structure and between the polar tube coils and the nucleus (Figs 60, 61).

DISCUSSION

Taxonomic considerations

***Tuzetia weidneri* sp. n.**

Baxter *et al.* (1970) briefly described a microsporidium which they named *Pleistophora* sp. in *L. setiferus* and *F. aztecus* and illustrated large "cysts" packed with spores, which were clear and persistent both in the dab smears and striated muscle sections. No measurements were given. Although there have been subsequent findings of *Pleistophora* in the same hosts (Constransitch 1970, Overstreet 1973), the species has not been named and there has been no formal description at light- or electron-microscopic levels. In the present ultrastructural study, it was clear that the microsporidia which developed in SVs did not belong to *Pleistophora*. Although the sporonts were multinucleate within SVs, the vesicles divided together with the sporont, so that each sporoblast lay in its own SV. Spores were thus loosely adherent in degraded host tissue, not aggregated in defined packets. Also, there was a tendency for the sporoblasts to be produced linearly, rather than in spherical groups. It is, thus, highly unlikely that the species we have described is the same as the *Pleistophora* sp. of Baxter *et al.* (1970) and we consider that it has not been described previously. Notable features of the mature SVs of *T. weidneri* were the absence of metabolic products (granules and tubules) and a complex pattern of ridges on the spore wall. Although *Pleistophora* sp. with persistent SVs as described by Baxter *et al.* (1970) has been found periodically in shrimp throughout the northern Gulf of Mexico (e.g. Overstreet 1973), it has not been collected by the authors off Mississippi for over 7 years.

Four genera, *Tuzetia*, *Janacekia*, *Alfvenia* and *Nelliemelba*, have been established for microsporidian species in which spores lie individually in SVs (Larsson 1983). The morphology of the microsporidia in *L. setiferus* and *F. aztecus* most closely fits the characters of *Tuzetia*, namely nuclei unpaired in all stages of development, meronts and sporonts dividing into a small number (2-8) of products, spores oval or pyriform, polar tube isofilar and exospore thin and without stratification. Most species of *Tuzetia* have evenly distributed, persistent narrow tubules, of unknown function, traversing the SV connecting the spore wall with the SV envelope. The tubular/spherical secretions in the *Tuzetia*-like microsporidia in *L. setiferus* and *F. aztecus* are not evenly distributed and their role appears to be linked with division of the sporont and disappear during spore maturation. We have tentatively assigned the species to the genus *Tuzetia* in spite of the difference which exists between the episporontal secretions and although the prominent system of ridges on the spore wall is a new feature for the genus. The only named species of *Tuzetia* that lacks episporontal tubules in mature SVs is *Tuzetia cyclopis* (Kudo 1921), named from the copepods *Cyclops fuscus* by Kudo (1921) and *Megacyclops viridis* by Loubès (1979). Spores of *T. cyclopis* are larger (4.2-4.7 x 2.7-3.0 μm) than those of *T. weidneri* and typically have 13 rather than 9-10.5 coils of the polar tube. For these reasons we have established *T. weidneri* as a new species. Also decapod crustaceans are new hosts for the taxon *Tuzetia*. As no difference was found in the *Tuzetia*-like microsporidia in their development and spore structure in *L. setiferus* and *F. aztecus*, material from both hosts is considered conspecific.

Taxonomic summary

***Tuzetia weidneri* sp. n.**

Type host: *Litopenaeus setiferus* (Linnaeus, 1767).

Other host: *Farfantepenaeus aztecus* (Ives, 1891).

Site of infection: striated muscle.

Type locality: Bayous associated with Mississippi Sound, Mississippi, U.S.A.

Diagnosis: nuclei always unpaired. Meront surface with a profusion of blisters which appear to be involved in division of the meront, usually into linear arrays of merozoites. Sporonts, which are enveloped by a fine sporophorous vesicle formed by fusion of the blisters at the surface of uninucleate or multinucleate stages, become rounded sporogonial plasmodia with a small number of nuclei. Sporonts become elongate and divide, together with the sporophorous vesicle, into linear arrays of sporoblasts each enveloped in its own sporophorous vesicle. Aggregates of globules and tubules secreted into the episporontal space are massed at the division planes

and are included in the sporophorous vesicles around sporoblasts. These secretions are degraded and disappear at spore maturity.

Spores are pyriform and measure 2.8-4.7 µm (m = 3.3 ± 0.1 µm) x 0.9-3.7 µm (m = 2.3 ± 0.1 µm) when fresh. Polaroplast has an anterior region of close-packed lamellae and a spongiform region around the posterior two thirds of the straight part of the polar tube. Polar tube is isofilar with 9-10.5 coils in a single rank close to the spore wall. Large posterior vacuole with flocculent contents. Spore wall ornamented with complex anastomosing ridges incorporating the endospore and the finely granular, non-stratified exospore.

Type material: resin blocks deposited in the University of Southern Mississipi Gulf Coast Research Laboratory Museum, Holotype - GCRL 2032 (from *L. setiferus*); paratypes GCRL 2033-2034 (from *L. setiferus*) and GCRL 2035-2037 (from *F. aztecus*)

Etymology: the specific name "*weidneri*" is proposed in honour of the contribution to microsporidiology of Professor Earl Weidner.

Perezia nelsoni

Perezia nelsoni was first described as *Nosema nelsoni* from *F. aztecus* collected from the Lousiana coast, USA (Sprague 1950). It has also been reported from *Litopenaeus setiferus* and *Farfantepenaeus duorarum* from coastal waters of the southern USA and from South Africa (summarised by Sprague and Couch 1971 and by Overstreet 1973) and later in *Parapenaeus longirostris* from the Mediterranean (Loubès *et al.* 1977), *Penaeus semisulcatus*, *Fenneropenaeus merguiensis* and *Penaeus esculentus* from Australia (Owens and Glazebrook 1988) and *Farfantepenaeus notialis* from Senegal (Clotilde-Ba and Togubaye 1995, 1996). The spore dimensions (measured fresh or fixed), provided by several authors are in accord with 2.5 x 1.5 µm given in the original description (Sprague 1950). The numbers of coils of the polar tube given by various authors are also within an acceptable range for a species i.e. 13 (Sprague 1977), 9-12 (Sprague and Vernick 1969), 8-13 (Loubès *et al.* 1977) and 10-11 (Clotilde-Ba and Togubaye 1995, 1996). In the present study the spore dimensions were 2.1 x 1.2 µm and the number of polar tube coils was 8-10. It is likely that *P. nelsoni* has a worldwide distribution, in a wide range of penaeid hosts but confirmation of this will rest with molecular studies.

Our studies of *P. nelsoni* have revealed merogonic stages with diplokarya and sporogonic stages with unpaired nuclei, in accord with the descriptions from *P. longirostris* (see Loubès *et al.* 1977) and *F. notialis* (see Clotilde-Ba and Togubaye 1996). However, we have been able to add more information on spore structure, the most interesting feature being the outer region of polaroplast, which in almost all of our specimens appeared as a globular sac composed of compact membranes enclosing the inner polaroplast, which in turn surrounded the straight part of the polar tube. In only two spores that we observed was the outer region seen to be open to the posterior part of the spore housing the nucleus and posterior vacuole. Although the outer polaroplast generally appeared mottled, with electron-dense and lucent parts, there were regions with traces of parallel membranes, and we have concluded that this part of the polaroplast had suffered fixation problems, disrupting the close-packed lamellae, thereby releasing the matrix that is normally enclosed by the membranes, and that the matrix had then become flocculent. We are fully in agreement with Clotilde-Ba and Togubaye (1996) that both polaroplast regions are composed of lamellae. These authors described the outer lamellae as being "anterior and lateral" but their illustrations clearly show the outer lamellae as encircling the inner, widely-spaced lamellae.

The closed sac appearance of the outer region is in accord with some images of *P. nelsoni* published by Sprague & Vernick (1969) i.e. Figs 4, 7, although unfortunately the enlargement (their Fig. 6), which might have shown whether the outer membranes are open or closed, does not extend to the posterior limit of the polaroplast. The organisation of the polaroplast of *P. nelsoni* is unusual but is similarly constructed in images of the closely-related species *Ameson michaelis* from crabs, *Callinectes sapidus* (see Sprague *et al.* 1968, Figs 10, 11 and Weidner 1970, Fig. 14d). Sprague *et al.* (1968) had first interpreted the outer polaroplast region as a fluid filled cavity and this appeared both closed (their Fig. 11) and open (their Fig. 12). This opinion was revised by Sprague and Vernick (1969) who proposed that it corresponded to the outer polaroplast zone of *P. nelsoni* and was thus a finely laminated structure. Weidner (1970) described the polaroplast of *A. michaelis* as spirally arranged. Larsson (1986) reviewed the range of polaroplast types in microsporidia. A polaroplast with a membranous inner component, enclosed by close-packed membranes forming a complete sac breached only by the polar tube, has not been described except in *Ameson* spp. and *P. nelsoni*.

Nosema nelsoni (Sprague, 1950) was transferred to the genus *Ameson* by Sprague (1977), then to *Perezia*

by Vivarès and Sprague (1979). The genus *Ameson* was established for *Nosema michaelis* by Sprague (1977) and differentiated from *Nosema* by its production of sporoblasts in chains from a moniliform multinucleate sporont, as opposed to production of sporoblasts in pairs from a binucleate sporont in *Nosema*. *Ameson* was placed in the family *Nosematidae* in the mistaken belief that sporoblasts (and presumably spores) were diplokaryotic (Sprague, 1977). This was later corrected (Vivarès and Sprague 1979). Two features, common to *A. michaelis* and *A. pulvis*, the latter species also from crabs (*Carcinus maenas*) described by Vivarès and Sprague (1979), are the outer region of compact polaroplast membranes and a layer of "bristles" covering the surface of sporoblasts and spores (Sprague *et al.* 1968, Vivarès and Sprague 1979). The transfer of *A. nelsoni* to *Perezia* was based on the absence of these bristle-like structures. However, the polaroplast of *Perezia lankesteriae* apparently lacks the outer region of close-packed membranes (Ormières *et al.* 1977) and, in this respect, *P. nelsoni* more closely resembles *Ameson* spp.

The present ultrastructural studies of *P. nelsoni* and *T. weidneri* have provided data which are in accord with the phylogenetic relationships of these species indicated by 16S rDNA sequences (Cheney *et al.* 2000). In their parsimony tree the species listed as *Pleistophora* sp. LS was most closely related to *A. michaelis*. As *Pleistophora* sp. LS has now been identified as *Perezia nelsoni*, the anomaly of a spieces thought to have SVs and *A. michaelis* without SVs within the same clade has been removed. Whether the presence or absence of hair-like projections on the spores carries sufficient weight to separate *P. nelsoni* on the one hand and *A. michaelis* and *A. pulvis* on the other hand into different genera is debatable, considering the extraordinary similarity in their merogonic and sporogonic stages and internal spore structure and given that they all parasitise decapod crustaceans. *Perezia lankesteriae*, a hyperparasite of the gregarine *Lankesteria ascidiae* in the ascidian *Ciona intestinalis*, may well be different but needs re-examination to reveal its mature spore structure.

The molecular study by Cheney *et al.* (2000) included the microsporidium, thought to be *Pleistophora* sp. from *F. aztecus*. This species, referred to as *Pleistophora* sp. PA, fell into a polytomy with *Glugea atherinae*, *Loma* sp., *Ichthyosporidium* sp. and *Loma acerinae*. In the present study it has been placed in the genus *Tuzetia* as *T. weidneri*, although it exhibited some morphological features not previously reported for the genus. No other species of *Tuzetia* has been examined for its 16S rDNA sequence so that the relationships of the type species *Tuzetia infirma* from the copepod *Cyclops fuscus* are unknown. *Janacekia debaisieuxi* is another species in which spores lie individually in SVs. It was split from the genus *Tuzetia* by Larsson (1983) because it is diplokaryotic in merogony and undergoes meiosis before producing uninucleate spores. *J. debaisieuxi* was found to be distant from *T. weidneri* (*Pleistophora* sp. PA) in the molecular study of Cheney *et al.* (2000). This adds credence to systematics which give weight to nuclear phenomena, especially diploidy and the occurrence of meiosis, in considering relationships among taxa (Sprague *et al.* 1992).

Acknowledgements. We thank Trish Rowland from Withington Hospital, Manchester for assistance with electron microscopy and Ronnie Palmer, Susan Plourde, Pam Monson, Kristine Wilkie, Marie Wright, Susan Carranza, Nate Jordan, Jody Peterson and Lex Galle (all from the University of South Mississippi) for collection and preparation of material from infected shrimps. The study was conducted in part under U.S. Department of Agriculture, Cooperative State Research Service Grant No. 98-38808-6019.

REFERENCES

Baxter K. N., Rigdon R .H., Hanna C. (1970) *Pleistophora* sp. (Microsporidia: Nosematidae): a new parasite of shrimp. *J. Invertebr. Pathol.* **16:** 289-291

Canning E. U., Hazard E. I. (1982) Genus *Pleistophora* Gurley 1893, an assemblage of at least three genera. *J. Protozool.* **29:** 39-49

Cheney S. A., Lafranchi-Tristem N. J., Canning E. U. (2000) Phylogenetic relationships of *Pleistophora*-like microsporidia based on small subunit ribosomal DNA sequences and implications for the source of *Trachipleistophora hominis* infections. *J. Eukaryot. Microbiol.* **47:** 280-287

Clotilde-Ba F.-L., Togubaye B. S. (1994) Ultrastructure and development of *Agmasoma penaei* (Microspora, Thelohaniidae) found in *Penaeus notialis* (Crustacea, Decapoda, Penaeidae) from Senegal. *Eur. J. Protistol.* **30:** 347-353

Clotilde-Ba F.-L., Togubaye B. S. (1995) Occurrence of microsporidia and gregarines in the shrimp *Penaeus notialis* from Senegal (West Africa). *Bull. Eur. Ass. Fish Pathol.* **15:** 122-124

Clotilde-Ba F.-L., Togubaye B. S. (1996) Complementary data on the cytology of *Perezia nelsoni* (Sprague, 1950) Vivarès and Sprague 1979 (Microspora, Pereziidae) found in *Penaeus notialis* (Crustacea, Decapoda) from Senegal. *Zool. Beitr. N. F.* **37:** 41-48

Constransitch M. J. (1970) Description, pathology and incidence of *Plistophora penaei* n. sp. (Microsporidia, Nosematidae), a parasite of commercial shrimp. Masters Thesis, Northwestern State University, Natchitoches, Louisiana

Couch J. A. (1978) Diseases, parasites and toxic responses of commercial penaeid shrimps of the Gulf of Mexico and South Atlantic coasts of North America. *Fish. Bull.* **76:** 1-44

Couch J. A. (1983) Diseases, caused by Protozoa. In**:** The Biology of Crustacea: Pathobiology, (Ed. A. J. Provenzano). Academic Press, New York, **6:** 79-111

Hazard E. I., Oldacre S. W. (1976) Revision of Microsporidia (Protozoa) close to *Thelohania*, with descriptions of one new family, eight new genera, and thirteen new species. U.S. Dept. of Agriculture Technical Bulletin No. 1530, 1-104

Kudo R. (1921) Microsporidia parasitic in copepods. *J. Parasitol*. **7:** 137-143

Larsson R. (1983) A revisionary study of the taxon *Tuzetia* Maurand, Fize, Fenwick and Michel, 1971 and related forms (Microsporidia, Tuzetiidae). *Protistologica* **19:** 323-355

Larsson R. (1986) Ultrastructure, function and classification of Microsporidia. *Prog. Protistol.* **1:** 325-390

Loubès C. (1979) Ultrastructure, sexualité, dimorphisme sporogonique des Microsporidies (Protozoaires). Incidences taxonomiques et biologiques. Thesis, Academie de Montpellier, Université des Sciences et Techniques du Languedoc, France

Loubès C., Maurand J., Comps M., Campillo A. (1977) Observations ultrastructurales sur *Ameson nelsoni* (Sprague, 1950) Microsporidie parasite de la crevette *Parapenaeus longirostris* Lucas consequences taxonomiques. *Rev. Trav. Inst. Pêches marit.* **41:** 217-222

Ormières R., Loubès C., Maurand J. (1977) Etude ultrastructurale de la Microsporidie *Perezia lankesteriae* Léger et Duboscq 1909, espèce-type: validation du genre *Perezia*. *Protistologica* **13:** 101-112

Overstreet R. (1973) Parasites of some penaeid shrimps with emphasis on reared hosts. *Aquaculture* **2:** 105-140

Owens L., Glazebrook J. S. (1988) Microsporidiosis in prawns from Northern Australia. *Aust. J. Mar. Freshw. Res.* **39:** 301-305

Sprague V. (1950) Notes on three microsporidian parasites of decapod Crustacea of Louisiana coastal waters. *Occ. Pap. Mar. Lab. Louisiana State Univ.* **5:** 1-8

Sprague V. (1977) Classification and phylogeny. In**:** Systematics of the Microsporida, Comparative Pathobiology (Eds. L.A. Bulla and T.C. Cheng). Plenum Press **2:** 1-30

Sprague V., Couch J. (1971) An annotated list of protozoan parasites, hyperparasites and commensals of decapod Crustacea. *J. Protozool*. **18:** 526-527

Sprague V., Vernick S. H. (1969) Light and electron microscope observations on *Nosema neloni* Sprague, 1950 (Microsporidia, Nosematidae) with particular reference to its Golgi complex. *J. Protozool.* **16:** 264-271

Sprague V., Becnel J. J., Hazard E. I. (1992) Taxonomy of phylum Microspora. *Crit. Rev. Microbiol.* **18:** 285-395

Sprague V., Vernick S. H., Lloyd B. J. (1968) The fine structure of *Nosema* sp. Sprague, 1965 (Microsporidia, Nosematidae) with particular reference to stages in sporogony. *J. Invertebr. Pathol.* **12:** 105-117

Vivarès C.P., Sprague V. (1979) The fine structure of *Ameson pulvis* (Microspora, Microsporida) and its implications regarding classification and chromosome cycle. *J. Invertebr. Pathol.* **33:** 40-52

Weidner E. (1970) Ultrastructural study of microsporidian development. I. *Nosema* sp. Sprague, 1965 in *Callinectes sapidus* Rathbun. *Z. Zellforsch.* **105:** 33-54

Received on 23rd July, 2001; accepted on 16th November, 2001